Air Quality, Atmosphere & Health (2021) 14:1969–1988
https://doi.org/10.1007/s11869-021-01069-9

The air pollution modelling system URBAIR: how to use a Gaussian model to accomplish high spatial and temporal resolutions

A. P. Fernandes[1] · S. Rafael[1] · D. Lopes[1] · S. Coelho[1] · C. Borrego[1] · M. Lopes[1]

Received: 22 January 2021 / Accepted: 21 July 2021 / Published online: 6 August 2021

Abstract
A current challenge in the environmental sciences field is to assess air quality at larger urban areas with high level of spatial resolution and, at the same time, with feasible computational resources time demand. This study provides a sensitivity analysis, focused on the implications of different grid resolutions on air quality results, followed by a performance assessment of the URBan AIR (URBAIR) model, a second-generation Gaussian model, as a tool for air quality management in urban areas. Estarreja area, a city located near an industrial complex, was used as case study, and the most critical air pollutants were investigated: particulate matter (PM10) and nitrogen dioxide (NO_2). Three different grid resolutions were tested: 0.1 km, 0.2 km and 0.3 km resolutions. Comparative results revealed that all grids provide similar results regarding the spatial distribution of PM10 and NO_2 concentrations, with evident differences in the magnitude of those concentrations and in the required computational time. The source apportionment analysis revealed the great contribution of industrial sources and road transport to NO_2 and PM10 concentrations, respectively. The URBAIR model is a useful tool to support decision-makers since it considers the specific characteristics of each city, which make it particularly helpful to assess different origins of air pollution, and so, to select the most effective sectorial measures that should be applied to improve local air quality.

Keywords Air quality management · Gaussian model · Model evaluation · Urban scale

Introduction

The dispersion of air pollution in urban areas has been of great concern in the scientific community in last decades. Despite some improvements, thanks to the implementation of European legislation on atmospheric emissions and air quality, key air quality standards for the protection of human health are, currently, not being achieved in a set of air quality monitoring stations across Europe (EEA 2019). This is particularly true for urban areas, where more than 70% of the European population lives (Rafael et al. 2018). Air pollution is still one of the greatest challenges of our time and its effects undermine the ability of cities to achieve sustainable development. The 2030 Agenda for Sustainable Development comprises 17 goals (United Nations 2015), where the commitment to make cities resilient and sustainable is included. It is a target of this goal, by 2030, to reduce the adverse per capita environmental impact of cities, by paying special attention to air quality.

Since 2008 with the publication of the European Air Quality Directive (AQD) (2008/50/EC), the use of models in combination with monitoring data has been encouraged for a set of applications. The air quality models to be applied depends on the temporal and spatial scale (from global to local scales), characteristics of the domain (size and resolution), the structure of the emission field (spatial and temporal distribution by emission sector), the air pollutants that will be simulated and on the application where the modelling results are to be used (Pianosi et al. 2016). Gaussian models have been widely used in atmospheric dispersion modelling, usually for regulatory purposes due to their easy implementation and their near real-time response.

A set of Gaussian models are currently available (e.g. CALINE4 (Benson 1989), CALPUFF (Scire et al. 1990a, 1990b), AERMOD (Cimorelli et al. 2005), UK-ADMS (Carruthers et al. 1994)) with a large set of applications. The studies that use Gaussian models on atmospheric modelling can be categorized in three main approaches:

✉ S. Rafael
sandra.rafael@ua.pt

[1] CESAM & Department of Environment and Planning, University of Aveiro, Aveiro, Portugal

i. studies that aim to provide a scientific review of the most common models and their applications; this type of studies discusses the specific requirements and limitations of a given model (related to the spatial and temporal resolution, the type of environment, the structure of the emission field and the pollutant compounds to be analysed) that can include model intercomparison (related to model's intrinsic simplifications and parametrizations and their performance) (e.g.Gulia et al. 2015; Oleniacz and Rzeszutek 2018);
ii. studies that aim to characterize the air quality status; this type of studies includes assessments for regulatory and industry purposes (e.g. impact and health risk investigations) and air quality assessment in urban areas using specific case studies to investigate different air quality problems (e.g.Borrego et al. 2016; Truong et al. 2016; Wu et al. 2018); the majority of these studies also assess the model capability and accuracy by comparison of modelled results with measured data;
iii. studies that aim to support decision-making in the design and implementation of urban policies; this type of studies includes the investigation of effectiveness of emission abatement strategies to improve air quality (e.g. Mocerino et al. 2020) or the evaluation of different types of urban structures as a response to environmental sustainability issues promoted by climate change and growing cities (e.g. Ma et al. 2013).

Despite the complexity behind the development of the air quality models, their results have a definite uncertainty, which is usually associated with input data (meteorological conditions and emissions rates) used in those models (Taghavi et al. 2005). Beyond that, some studies have been showing that model results are considerably sensitive to grid resolution (Pianosi et al. 2016). The studies conducted agree in their main conclusions: a coarse grid resolution may produce large discrepancies in the results compared to a fine grid resolution since it cannot capture inhomogeneity in emission rates, meteorology and land use; a fine grid may cause the simulation to be inefficient since it can be considerably limited by calculation time (Garcia-Menendez and Odman 2011; Fountoukis et al. 2013). Therefore, air quality studies should be performed using the appropriate grid resolution to obtain reliable and acceptable results in terms of both accuracy and computational time, selected according to the study scope.

Given this background, there is a question that has not been explored yet: how a regional approach can be applied and optimized in Gaussian models to achieve an air quality assessment with high level of spatial and temporal resolution? To answer this question, this work presents a case study application of URBAIR model over the Estarreja area, in Aveiro region (Portugal), based on the use of detailed atmospheric emission inventory (in gridded format). The applied approach allows to achieve two main goals: (i) to assess the influence of different spatial resolutions on model predictions; and (ii) to evaluate the contribution of different emission sources to local air pollution. The atmospheric dispersion of nitrogen dioxide (NO_2) and particulate matter (PM10), both pollutants posing serious health concerns in urban areas, is analysed.

The paper is structured as follows: section 'Modelling approach' describes the methodology, including a brief description of the modelling architecture and the approach applied to model evaluation. The modelling application and the main results are presented in section 'Case study—air quality assessment', including the model sensitivity analysis and source apportionment results. Conclusions follow in section 'Conclusions'.

Modelling approach

This section provides an overview of the modelling approach used to characterize the air quality at the urban scale, which includes a detailed description of the air quality modelling system URBan AIR (URBAIR) (section 'Modelling setup') and a description of the methodology applied to evaluate the model sensitivity and model performance to a set of parameters (section 'Model evaluation').

Modelling setup

The URBAIR model is an improved version of the second-generation Gaussian model POLARIS Gaussian plume dispersion model (Borrego et al. 1997). This modelling system is designed to be modular and includes the pre-processing of land use and urban elements geometry, meteorological conditions and air pollutant emissions, coupled with a dispersion module. The URBAIR provides air quality patterns for a given spatial domain (with up to about 50 km from the domain centre) and time period (e.g. hourly, daily, 1 year or multiple years) for different air pollutants, namely PM10, NO_2, SO_2 and CO. The system framework is designed in a way that the inputs/outputs of the different modules are shared and linked along the modelling process. URBAIR's structure is organized as schematically shown in Fig. 1. The four main modules composing the URBAIR system are hereafter described.

The model was developed in the scope of the BRIDGE project (Chrysoulakis et al. 2013) where it was applied to assess the impact of different urban planning alternatives on air quality. Since then, the URBAIR has been implemented

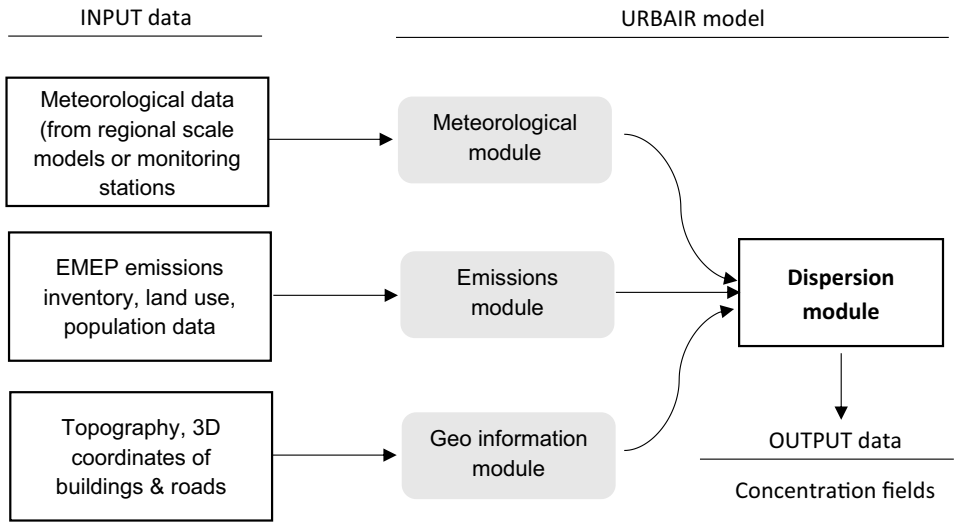

Fig. 1 URBAIR modelling system architecture

for a set of urban applications (Borrego et al. 2016; Dias et al. 2018) and tested against measured data.

Meteorological module

The main outcome of this module is to characterize the dynamics of the atmospheric boundary layer (ABL) during the period of simulation and pre-process relevant meteorological parameters for the dispersion module, following the Monin–Obukhov similarity theory approach (Tavares et al. 2011). This module uses surface and upper air (soundings) meteorological databases provided by regional scale meteorological models, or alternatively, by measurements. The main outputs consist of ABL turbulence scaling parameters (such as Monin–Obukhov length scale, surface friction velocity or convective velocity scale) and the mixing height of the ABL. The Weather Research and Forecasting (WRF) mesoscale model has been used to initialize the URBAIR model rather than measured data, since there are relatively few meteorological stations in Portugal with vertical profile information. The WRF model, from the National Center for Atmospheric Research (NCAR) (Skamarock et al. 2008), version 3.7., is a mesoscale numerical weather prediction system designed to serve both operational forecasting and atmospheric research needs. The WRF model is widely applied, has been extensively tested and shown to produce robust and realistic results (Rafael et al. 2020, 2019, 2018; Lopes et al. 2019).

Emissions module

The URBAIR has the capability of consider different types of emission sources, namely, area, volume, point (such as industrial) and line sources (road traffic emissions). The model also offers the possibility of prescribing the emission rate considering the temporal and spatial patterns of the emission sources. Recent developments in this module have been performed to allow the use of emissions in a grid format, able to use data from emission inventories, obtained either by using bottom-up or top-down approaches, which are usually used in chemical transport models for regional studies. This development allows the application of URBAIR model to urban domains with a finest resolution (tens of meters) that is not achieved in regional air quality models. As a result, a sensitivity analysis to the use of different grid resolution and its influence on air pollutant concentrations, the focus of this study, is required.

Geo-information module

The URBAIR model requires the characterization of the terrain surface elevation, land use, buildings 3D coordinates and emission sources location and dimension, to realistically represent the topography and build-up structures. This module relies on a Cartesian coordinate system, in which regular and discrete gridded data can be used to input and spatially distribute terrain and obstructions, receptors and sources within the simulation domain. Topography is specified in the form of terrain heights at receptor locations. The influence of buildings on air pollutant dispersion depends on the orientation of the obstacles relative to the source, the wind direction and the shape of the building. Direction-specific downwash parameters, in the form of projected building height and width dimensions, are estimated using the EPA's Building Profile Input Program PRIME (BPIP-PRIME) modelling approach (Schulman et al. 2000). This module's input information can be provided by GIS-based maps in a compatible-format to be readily processed.

Dispersion module

The dispersion module has implemented an improved version of the second-generation Gaussian model POLARIS to estimate the air pollutant concentration. The module uses a steady-state multi-source plume air Gaussian dispersion modelling approach, where the effects of meteorological conditions, topography and the presence of buildings are considered for the transport and dispersion simulation of air pollutants within urban areas. Under stable ABL conditions, it assumes the concentration spatial distribution to be Gaussian in both vertical and horizontal lengths; whereas in convective conditions, the horizontal distribution is also assumed to be Gaussian, but the vertical distribution is described with a bi-Gaussian probability density function (e.g. Weil et al. 1997). The meteorological conditions are assumed to be steady during the modelling period steps (typically hourly) and horizontally homogeneous. Vertical variations can be also considered, if concentration fields are estimated at various levels. The influence of complex terrain is provided through the concept of a dividing streamline by combining a horizontal plume state and a terrain following state (Cimorelli et al. 2005). An additional feature is the capacity to account for the dispersive nature of the 'convective like' boundary layer that forms during night-time conditions over urban areas, by enhancing the turbulence resulting from urban heat flux, similarly to AERMOD model (Cimorelli et al. 2005). As outputs, the URBAIR provides the air pollutant concentration spatially distributed over a regular grid, and, if the user required it, the air pollutant levels for specified receptor points.

Model evaluation

Two different approaches were applied to evaluate the URBAIR model: (i) sensitivity analysis, to investigate how the variation in the numerical model outputs can be attributed to different computational grid resolutions; and (ii) assessment of model performance, by comparing modelled results against measurements (statistical metrics); this evaluation was only made for the most appropriate grid resolution, chosen accordingly to the sensitivity analysis results.

The sensitivity analysis was performed to assess the model response, in terms of computational time consumed and air quality levels (magnitude and trends), to three horizontal grid resolution: coarse (0.3×0.3 km^2), medium (0.2×0.2 km^2) and fine (0.1×0.1 km^2) mesh. These grids were set based on two criteria: (i) high-resolution, to guarantee the representative of urban phenomena on air quality assessment; (ii) compromise between the domain area, the time period and the spatial and temporal resolution. The model performance was evaluated applying the BOOT Statistical Model Evaluation Software Package (Chang and Hanna 2004). The model acceptance criteria proposed by Chang and Hanna (2004) for air quality models' assessment, establish performance measures for six statistical parameters: (i) the normalized mean square error (NMSE < 1.5) is a measure of scattering and reflects the systematic errors; (ii) the fraction of predictions within a factor of two of observations (FAC2 > 0.5) is the most robust statistic measure since it is not overly influenced by high and low outliers; (iii) the correlation coefficient ($r = 1$) reflects the linear relationship between two variables; (iv) the root mean square error (RMSE $= 0$) gives important information about the skill in predicting the magnitude of a variable; (v) the index of agreement ($d = 1$) provides a standardized measure of the degree of model prediction (Willmott 1981); and (vi) the mean bias error (MBE $= 0$) can indicate whether the model overestimates or underestimates the concentration values measured. All these statistical parameters were considered in the analysis. Time-series were generated to complement the statistical analysis. The statistical parameters were also used to quantitatively assess the differences between the grid resolutions.

Case study—air quality assessment

This section provides a description of the modelling setup applied to Estarreja area located on the northern of Aveiro region, Portugal (section 'Model application'), a sensitivity analysis of the modelled results to mesh resolution (section 'Sensitivity analysis') and an assessment of model performance (section 'Model performance'). An air quality assessment, aiming to characterize the air quality status of the study area (section 'Air quality assessment'), is also provided in this section.

The case study comprises an area of 13.4×16.8 km^2 with four industrial areas (Avanca, Estarreja, Cacia and Albergaria-a-Velha) with moderate Heavy-Duty Vehicles (HDV) traffic (Fernandes et al. 2019); hence, the air quality can represent an important issue, namely for PM10 and NO_2 concentrations. The Estarreja area is a very interesting case study in terms of air quality since it is influenced by a set of emissions sources (industrial, traffic and residential sources), which implies a challenge in terms of air quality management for the most critical pollutants at urban areas NO_2 and PM10.

Model application

The modelling system, composed by WRF/URBAIR, was applied to 1-year simulation (2017). The WRF model was applied to four online-nested domains with increasing resolution at a downscaling ratio of three. Figure 2a shows the model domain setup used, which is composed of a

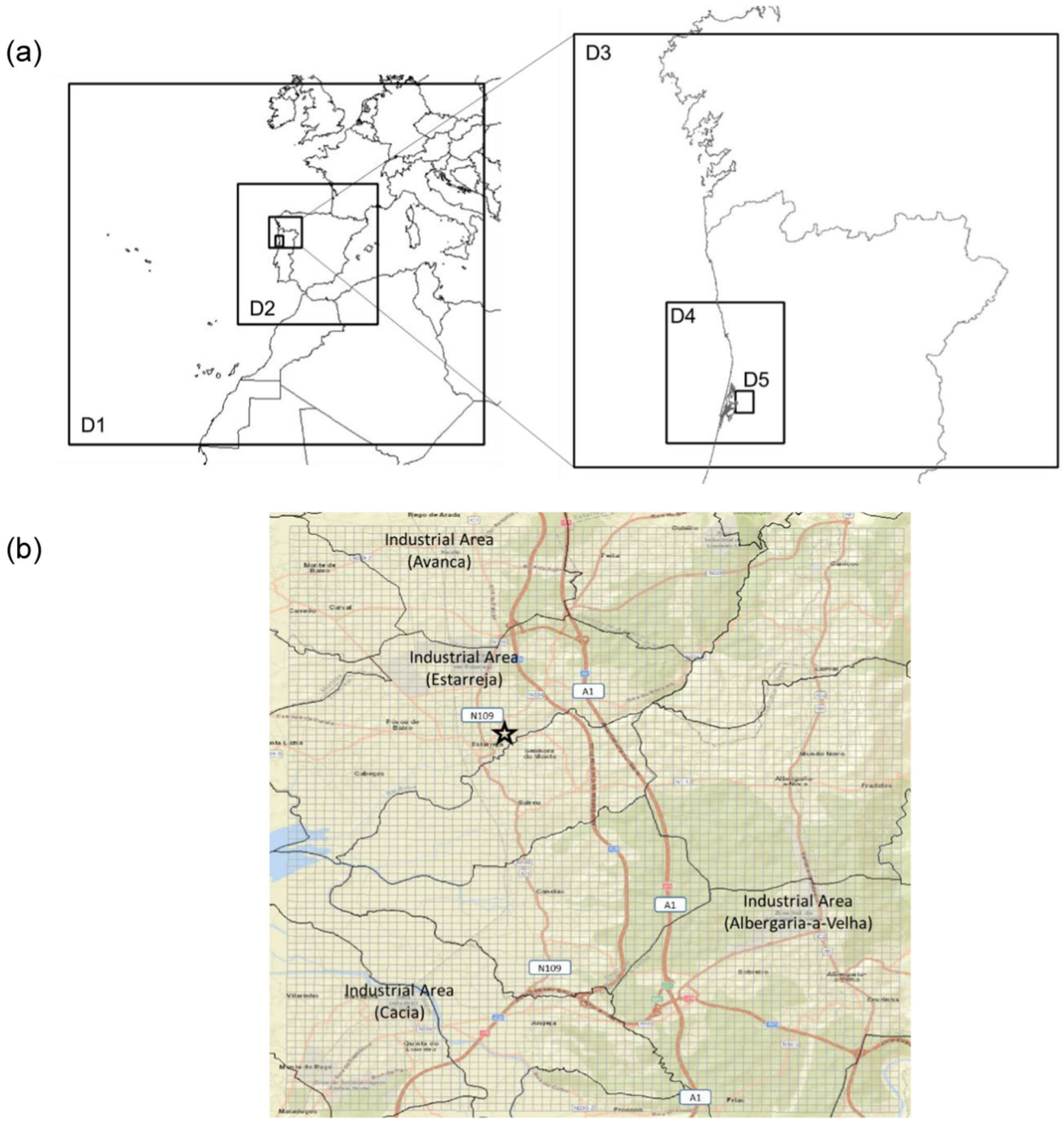

Fig. 2 **a** Configuration of the WRF model domains. Horizontal resolution of the coarse domain is 27 km, with 173 × 142 horizontal grid cells (D1). The inner WRF model domain has a horizontal resolution of 1 km with 94 × 163 horizontal grid cells (D4). The URBAIR model domain (D5) is also displayed. **b** Study domain showing the URBAIR computational domain with a spatial resolution of 0.2 km with 67 × 84 horizontal grid cells (grey lines), the parishes' limits that are within the study area (black lines), main roadways (orange lines) and location of the air quality monitoring station (star).

coarser domain of 27-km horizontal resolution covering part of Europe and part of the North of Africa (D1), and the innermost domain of 1-km horizontal resolution focusing on a confined area (D4), which comprises the Aveiro region. ERA-Interim analysis data (URL2), from the European Centre for Medium-Range Weather Forecasts (ECMWF), was used as initial and boundary conditions for WRF simulations at 6 h and 0.75° temporal and spatial resolution, respectively. The following set of parameterizations were used in the analysis: WRF Single-moment 5-class

Microphysical Scheme (Hong et al. 2004); Dudhia Shortwave radiation scheme (Dudhia 1989); RRTM (Rapid Radiative Transfer Model) longwave radiation model (Mlawer et al. 1997); MM5 similarity surface layer scheme (Zhang and Anthes 1982); Unified Noah Land Surface Model (Tewari et al. 2004); Yonsei University Planetary Boundary Layer scheme (Hong et al. 2006) and Grell 3D Ensemble Scheme for cumulus parametrization (Grell and Dévényi 2002). The selected parameterizations were based on recommendations included in Wang et al. (2014), as well as on validation and sensitivity studies previously performed over Portugal (Rafael et al. 2016, 2017, 2018) and over the Iberian Peninsula (Fernández et al. 2007).

The numerical simulation was based on the meteorological dataset for the year 2017. The URBAIR model was applied to a modelling domain that covers an area of about 13.4×16.8 km^2 under the industrial built-up area (D5), within the D4 domain. The domain comprises one air quality monitoring station based on the Portuguese air quality monitoring network stations; the locations of which are indicated in Fig. 2b. The application of URBAIR was applied for the entire 2017 year, being the analysis made in an annual and seasonal basis.

The URBAIR initial meteorological conditions were provided by WRF model, in particular, the surface and vertical temperature and wind velocity profiles. In order to enable the direct extraction of WRF output data, a post-processor was developed and implemented to prepare these data in a URBAIR-compatible format.

The characterization of the wind fields provided by the WRF model for Estarreja area, was performed through the representation of wind roses for all the year of 2017 (Fig. 3) and for each season (Fig. 4): spring (March–May), summer (June–August), autumn (September–November) and winter (December–February). Wind roses represent the wind intensity and wind direction, with the percentage of times, during the selected period, that the wind blows from the indicated direction. Thus, a typical North wind is represented in the wind roses in the upper quadrants.

The analysis of Fig. 3 shows that, for 2017, the most representative values of wind speed are between 0 and 6 m s^{-1}, representing 87% of the data. Relatively to the wind direction, the prevailing winds are from Northwest (NW). In more detail, about 45% of the wind records are from NW quadrant, 22% comes from Southeast (SE) quadrant, 21% from Northeast (NE) quadrant and, finally, 12% from Southwest (SW).

Figure 4 illustrates the seasonal variability of wind speed and direction for Estarreja area.

In spring, about 38% of the wind are from NW, with the most representative values of wind speed between 3 and 6 m s^{-1}, which are wind conditions very typical of West Portuguese coast. This phenomenon is even more evident

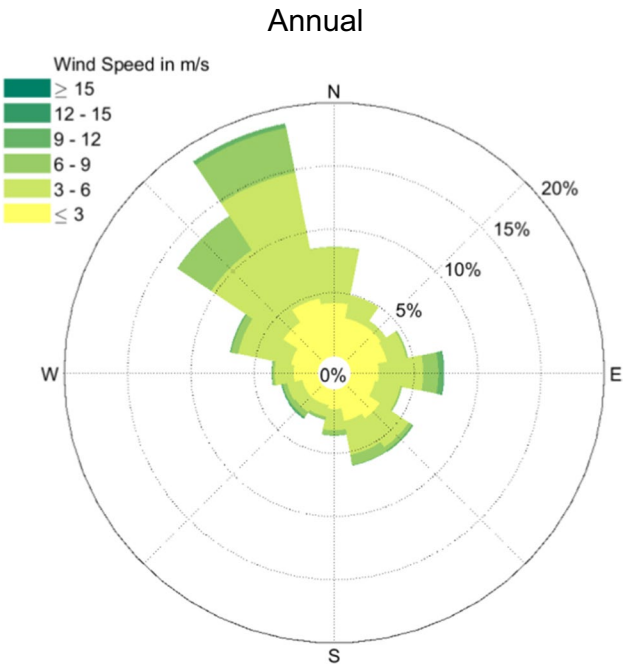

Fig. 3 Wind rose for all the year of 2017, for Estarreja area

in the summer months, with about 76% of winds coming from NW, with wind speeds up to 9 m s^{-1}. During these months, the wind that comes from South quadrants is typically weaker, with wind speed values below 3 m s^{-1}. The wind patterns obtained for autumn are quite similar to those obtained from spring, showing higher frequency of wind records from the NW quadrant. For the autumn months, 43% of the winds are from NW. However, in the winter months, the wind pattern is different from those obtained for the remaining seasons, with higher wind speed values, reaching 18 m s^{-1}. During winter, 31% of the wind comes from the SE quadrant, 30% from NE quadrant, 24% from NW quadrant and only 15% from SW quadrant.

The atmospheric emissions were obtained from the European Monitoring and Evaluation Programme (EMEP) (EMEP 2017). Since this inventory provides values with a coarse spatial (10×10 km^2) and temporal resolution (annual) different proxies were used to refine the following SNAPs (Selected Nomenclature for Air Pollution): SNAP (1) Power stations; SNAP (2) commercial and residential combustion; SNAP (3) industrial combustion, SNAP (4) production processes; SNAP (5) extraction and distribution of fossil fuels and geothermal energy; SNAP (6) solvent and other product use; SNAP (7) road transport; SNAP (8) other mobile sources and machinery; SNAP (9) waste treatment and disposal; and SNAP (10) agriculture.

Regarding the spatial distribution, land use data, population information, buildings shapes and atmospheric emissions, a bottom-up approach was used to provide values over

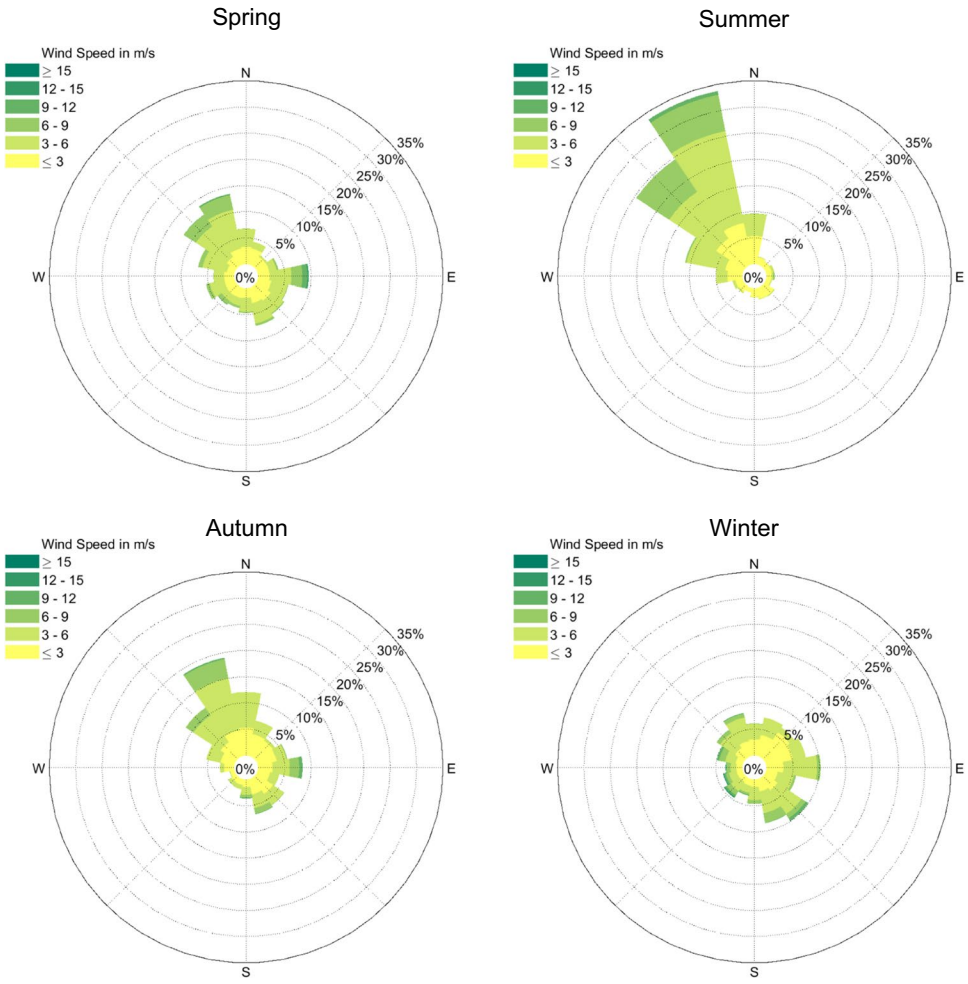

Fig. 4 Wind rose for each season of 2017, for Estarreja area

the study domain with high spatial resolution (hundreds of meters—100 m, 200 m and 300 m). For the industrial (SNAPs 3 and 4), off-road (SNAP 8), maritime transport (SNAP 8), waste treatment/disposal (SNAP 9) and agriculture (SNAP 10) sectors, the Portuguese land use data (DGT 2018) was considered. The study developed by Silveira et al. (2017) about how to build a high spatially resolved inventory for the residential combustion sector and population information from the Portuguese census dataset (INE 2011) was used to improve the emissions from commercial and residential combustion (SNAP 2). The OpenStreetMap (OpenStreetMap contributors 2017) data with the buildings shapes coordinates and the Transport Emission Model for Line Sources (TREM) (Li et al. 2019; Tchepel et al. 2012; Vicente et al. 2018) were considered, respectively, for the solvent and road transport activities.

The EMEP inventory was also adapted to generate hourly emissions to the study domain using the data from Gon et al. (2011) who provided typical European monthly, weekly and hourly profiles patterns for the main anthropogenic emission activities.

In order to analyse the atmospheric emissions over the study area, Fig. 5 shows the monthly contribution to the total emissions (in %) and the total emissions (in ton) of PM10 and NOx for each anthropogenic source. In addition, for the same air pollutants, the spatial distribution of annual emissions for the total and by main activities (residential combustion—SNAP 2; industries—SNAP 3 and SNAP 4; road transport—SNAP 7; other sectors—SNAP 6, SNAP8, SNAP 9, SNAP 10) is presented in Fig. 6.

The results show that the main anthropogenic emission sectors for both pollutants analysed are the industries (SNAP 3/4) and road transport (SNAP 7). The contribution of each activity to the total emissions recorded a slight variation between seasons.

For the PM10, the industries (SNAP 3/4; 89–97%), commercial and residential combustion (SNAP 2; 1–10%) are the main emission sources while the remaining activities (SNAP 6, SNAP 7, SNAP 8, SNAP 9 and SNAP 10) record a contribution of less than 1%. The highest SNAP 3/4 contribution is registered in summer while in the SNAP 2 is obtained in winter. The total emissions are higher in winter (391–418

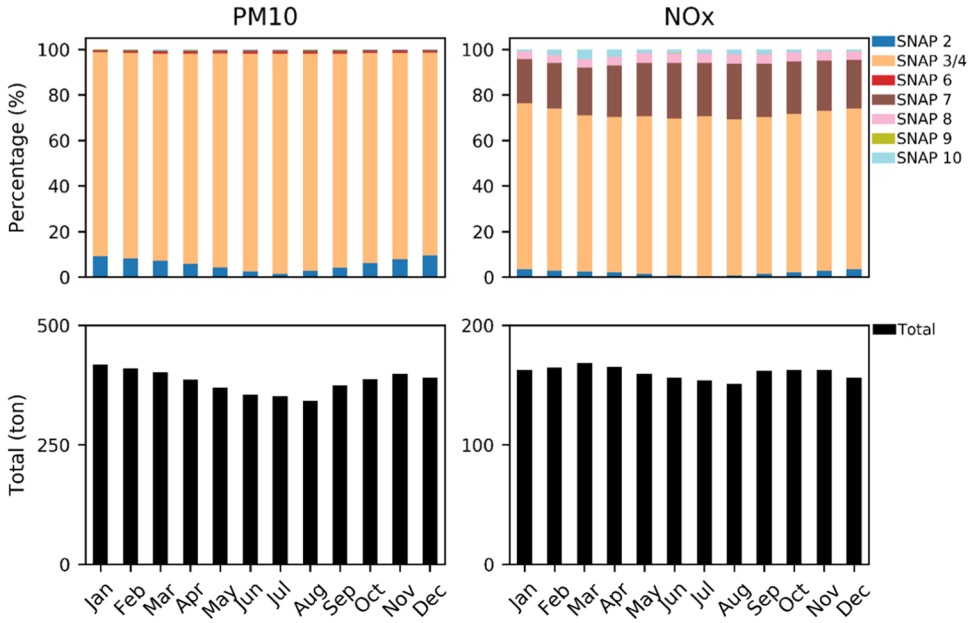

Fig. 5 Monthly emission shares by sector and the total values(in ton of pollutant) of PM10 and NOx in the study area

ton) followed by the autumn (374–399 ton), spring (370–402 ton) and summer (342–355 ton).

The industries (SNAP 3/4; 68.5–72.9%) and road transport (SNAP 7; 19.4–24.3%) are the main atmospheric sources of NOx. The sectors SNAP 6, SNAP 8 and SNAP 9 do not contribute for this pollutant emission while the remaining activities (SNAP 2, SNAP 8 and SNAP 10) have a contribution from 0.4 to 4.3 ton. The highest values are recorded in spring (159–169 ton), autumn (162–163 ton), winter (156–165 ton) and summer (151–156 ton).

The spatial distribution of PM10 and NOx (Fig. 6) is similar with higher emissions mainly over industrial areas of Avanca, Estarreja, Cacia and Albergaria-a-Velha, while for the remaining areas, the main sources are from residential (SNAP 2), road transport (SNAP 7) and other sectors (SNAP 6, SNAP 8, SNAP 9 and SNAP 10). In fact, only a small fraction of the study domain, over the Ria of Aveiro (Aveiro Lagoon), does not register any emission value.

For the residential combustion activity (SNAP 2), the highest emissions are recorded over the main urban areas of Albergaria-a-Velha (PM10 maximum = 1.3 ton; NOx maximum = 0.3 ton), Beduído (PM10 maximum = 0.9 ton; NOx maximum = 0.2 ton) and Cacia (PM10 maximum = 0.8 ton; NOx maximum = 0.1 ton). For the road transport sector, the maximum value is obtained, for both air pollutants, near N109 in Cacia (PM10 maximum = 0.6 ton; NOx maximum = 8.3 ton) while for the other sectors (SNAP 6, SNAP 8, SNAP 9 and SNAP 10), the Albergaria-a-Velha and Cacia parishes are more affected respectively, by PM10 (ranges from 9.0×10^{-6} to 0.1 ton) and NOx (varies between 0 and 0.1 ton) emissions.

Sensitivity analysis

The sensitivity analysis was conducted to assess how mesh resolution can influence air pollutant concentrations. It was also an aim of this analysis to choose the computational grid resolution that achieves a compromise between an accurate analysis and the demand of computational resources for a further air quality assessment. The analysis was conducted for 4 typical days (on an hourly basis)—weekday and a weekend from the winter season, and a weekday and a weekend from summer—and three grids were set: (i) coarse grid, with a resolution of 0.3×0.3 km^2 and a total of 2520 cells; (ii) medium grid, with a resolution of 0.2×0.2 km^2 and a total of 5628 cells; and (iii) fine grid, with a resolution of 0.1×0.1 km^2 and a total of 22,344 cells. The 4 typical days where selected using as criterion the emissions variability, aiming to guarantee that the selected days capture the emissions annual seasonality and the weekly variability. A detailed description of the method used to select the 4 typical days can be found in Kewo et al. (2020) and Rafael et al. (2021). All the inputs, namely the atmospheric emissions, were estimated taking into account the different mesh resolutions. This means that the spatial disaggregation of the base emissions (from EMEP inventory) was performed to the three mesh resolutions under analysis. Regarding the meteorological variables, the URBAIR model was initialized, for the three tested resolution grids, by using an average of the WRF cells values that overlap the URBAIR domain, with a spatial resolution of 1 km. The grid results were compared based on three parameters: (i) air pollutant concentration (maximum and average values); (ii) the spatial pattern of

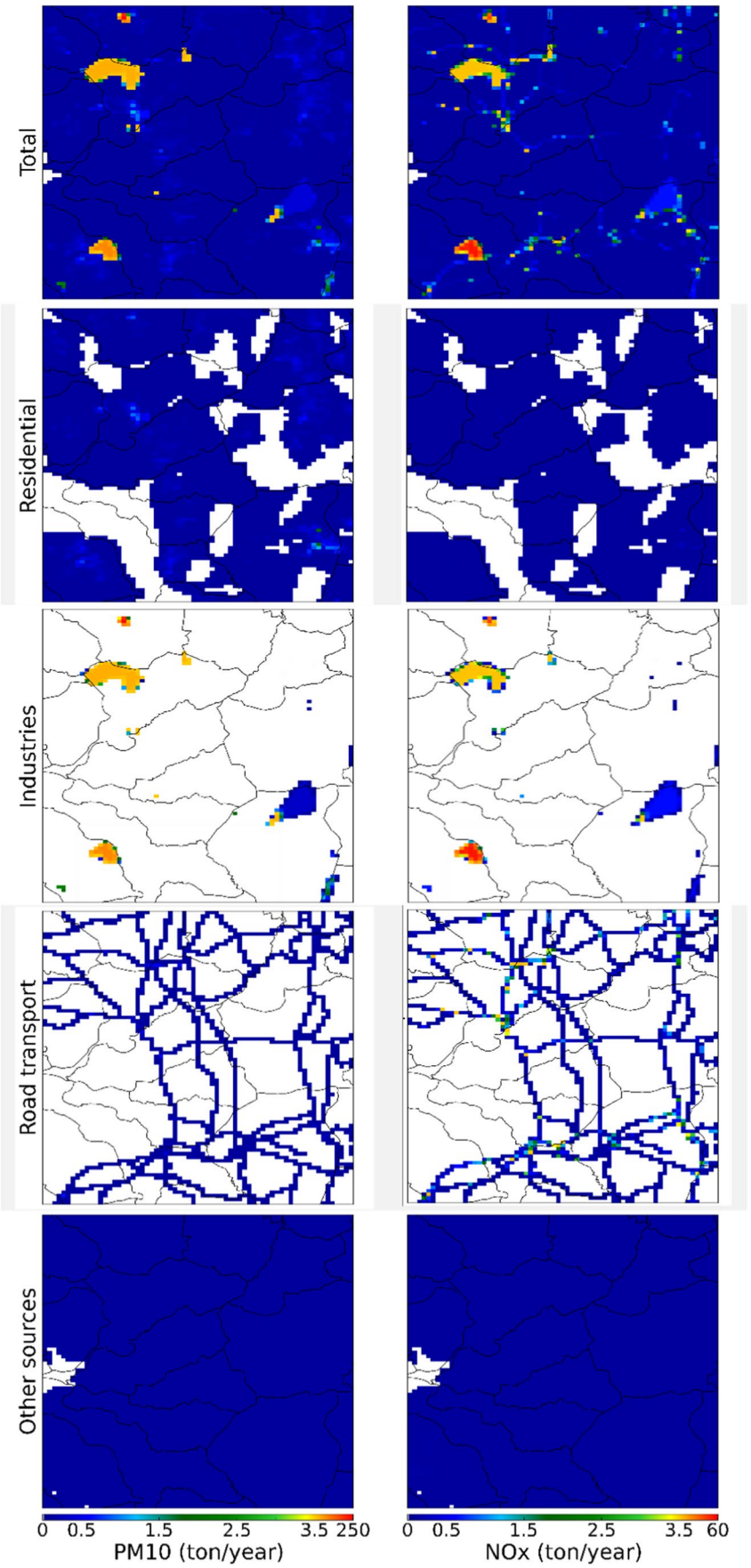

Fig. 6 Spatial distribution of PM10 and NOx emissions over the study area for the year 2017, considering a spatial resolution of 200 m. The areas bordered by grey lines represent the parishes' limits that are within the study area

air pollutant concentrations; and (iii) computational time required, which consisted in the quantification of the time spent in pre-processing, model running and post-processing.

The results showed differences between the coarse grid and the medium and fine grid, in all the analysed parameters, with these differences being similar for both PM10 and NO_2 pollutants, and for the 4 typical days analysed. As an example, PM10 results for 24-h average concentrations are presented and discussed. Figure 7a shows the spatial distribution of PM10 concentrations for the three grids under analysis, in a daily basis. Since the URBAIR model is a non-chemistry reactive model, the differences in the PM10 concentrations across the mesh resolutions (magnitude and spatial distribution) are mostly related with the level of detail of input data that is needed for each grid. As a result, the relative differences between grids (spatially and temporally), for the simulated days and pollutants considered, were constant.

Note that the simplified chemistry available in URBAIR model can be seen as a model limitation depending on the aim of the model application. Therefore, it is important to analyse the obtained results considering the reasons that underlie the adoption of a Gaussian model: (i) this work is focused on urban scale (spatial resolutions less than 1 km), which is very difficult to achieve with complex Chemistry Transport Models (e.g. CHIMERE and CAMx); (ii) mesoscale models do not take into account the phenomena that occur at the urban scale, while more detailed models such as Computational Fluid Dynamics models, due to their complexity, do not allow the simulation of large domains; and (iii) several authors point out Gaussian models as the tool to make the link between mesoscale and local scale and Gaussian models are widely recommended for regulatory use.

Regarding the spatial patterns of PM10 concentrations, all grid resolutions showed similar behaviour; however, the coarse grid fails to reproduce the hotspots modelled in both fine and medium grids, in terms of the hotspot coverage and its magnitude. This difference is particularly relevant since one of the main goals of an air quality modelling approach is to represent pollutant peaks and its location. The differences between the grid resolutions are highlighted through the analysis of the air pollutant concentrations (maximum and average values). Even though the average values (spatial averaged) are equally reproduced by all the grids, the magnitude of the maximum values differ between grids: 62 μg m^{-3} for the coarse grid, 78 μg m^{-3} for the medium grid and 82 μg m^{-3} for the fine grid. The medium and fine grids provide maximum values with a magnitude 5% and 25% higher than the coarse grid, for both PM10 and NO_2 concentrations. To explore with more detail the differences between mesh resolutions, a concentration-frequency distribution analysis was performed (Fig. 7b). Comparing the medium and fine grids, small differences in the PM10 daily average concentrations were obtained between them, with the fine grid providing, on average, air pollutant levels 0.2% higher. It can also be concluded that for all mesh resolutions,

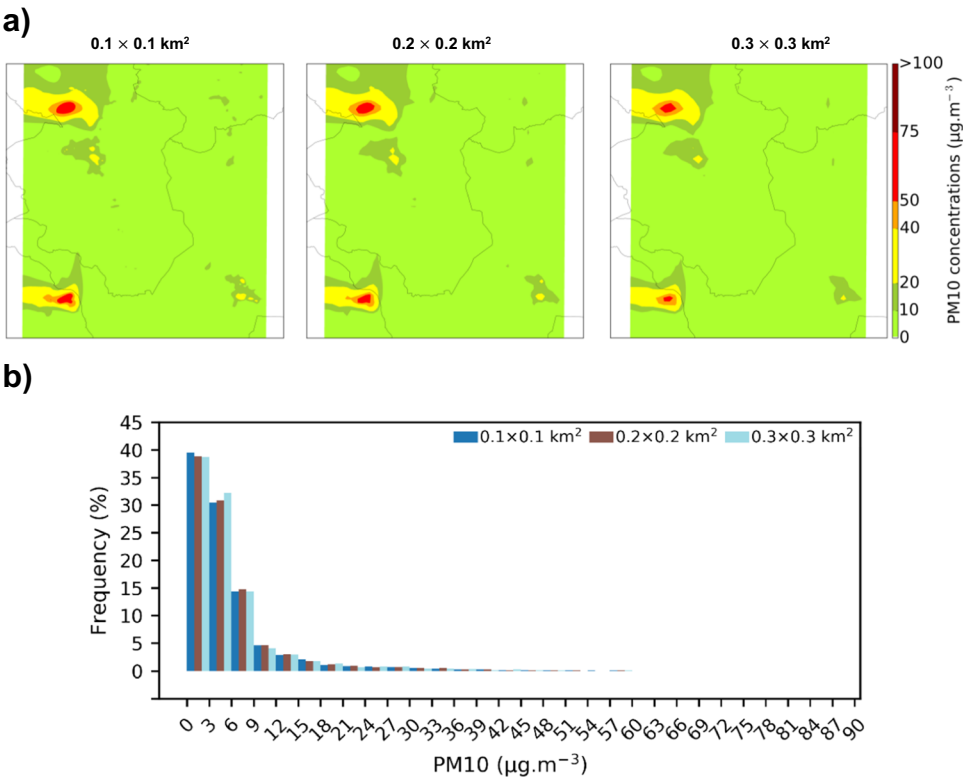

Fig. 7 Daily average PM10 concentrations for three different mesh resolutions: **a** Spatial distribution maps and **b** concentration-frequency distribution analysis

Table 1 Statistical comparison of the computational grid resolutions under analysis, considering the finest resolution results as reference

Grid resolution	NMSE (−)	*r* (−)	RMSE (μg m^{-3})	MBE (μg m^{-3})
0.3 vs 0.1 km	0.07	0.98	1.52	0.06
0.2 vs 0.1 km	0.03	0.99	1.00	-0.02

more than 50% of the cells of domain shows PM10 concentrations varying in a range of 0 and 9 μg m^{-3}. Beyond the differences in the magnitude of maximum PM10 concentrations, the area affected by high concentrations shown small differences independent of the mesh resolution; overall, the medium and fine grid showed high levels of PM10 concentration in an area similar to the coarse grid.

To conduct a more quantitative analysis of the grid differences, a set of statistical metrics were calculated (Table 1), considering the fine grid results as reference values. To provide a spatial comparison of the different mesh grids, a spatial join tool available in the geographic information system (GIS) software was applied. The spatial join tool allows joining attributes (in this case, PM10 and NO_2 concentrations) from one feature (medium and coarse grid resolution) to another (fine grid resolution) based on the spatial relationship, i.e. if a join feature has a spatial relationship with multiple target features, then it is counted as many times as it is matched against the target feature. A total of 22,344 receptors points (the number of cells of the fine grid) were used to compare the modelled results from different computation grid resolutions. The results showed that the medium grid has slightly higher value of the correlation factor (around 0.99) with the fine grid, when compared to the coarse and fine grid resolutions (0.98). The negative value of MBE indicated that medium grid underestimates the fine-grid concentration results. Distinguishable behaviour is obtained between the medium and coarse grids in terms of MBE. The positive value of MBE indicated that coarse grid overestimates the concentration results. Both NMSE and RMSE showed lower values when the medium and fine grids were compared than the ones obtained between the coarse and fine grids.

In relation to the computational time required to perform the modelling simulations, the analysis of the computational time demand was done by quantifying the run time versus number of sources (related to the mesh resolution), which provides an outlook of the amount of time only related to the model processing (software time demand).

All the URBAIR simulations were conducted considering the following hardware characteristics: 1 core and 8 GB of RAM. Table 2 shows the computational time required to perform the URBAIR simulations, considering all steps (pre-processing, model running and post-processing), for the different mesh resolutions. To simulate 24 h with a maximum of 22,258 sources (fine resolution), a time run of about 32 h was required (Table 2).

Table 2 Comparison of computational time required in URBAIR simulations (considering pre-processing, model running and post-processing) for different mesh resolutions, for a daily simulation (24 h)

	Mesh resolution			
		Coarse resolution	Medium resolution	Fine resolution
	Grid cells	2520	5628	22,344
	Number of sources	2515	5616	22,258
Computational time (minutes)	Pre-processing	120	120	120
	Model running	23	110	1898
	Post-processing	5	5	30
	Total	148	235	2048

Analysing all the modelling steps (pre-processing—inputs preparation, model running and post-processing—outputs representation), the results show that increasing grid resolution from the coarse resolution to the finest resolutions implies an increase in the computational time requirements (see Table 2). This increase is related with the amount of grid cells used in each mesh resolution. Considering the coarse grid as reference, the total computational time increases to 1.5 and to 13 times more, for the medium and fine grids, respectively. Looking individually for each step of the modelling application, the main differences between the grids were obtained in the modelling run and the post-processing analysis (this step takes 6 times more time for the fine grid by comparison with both coarse and medium grids). The time spent in the modelling run increase with the increment of spatial resolution, being responsible for 15.5%, 56.8% and 92.7% of the total computational time, for the coarse, medium and fine grids, respectively.

Figure 8 shows the linkage between the time demand and the number of sources used in the simulations. It seems that there is a linear relation between the number of sources considered in the model simulation and the computational time required, with the run time increasing notably with the increase of emission sources. An *R*-squared (statistical measure of how close the data are to the fitted linear trend line) of 0.99 was obtained, which means that regression model accounts for 98% of the variance. The more variance that is accounted for by the regression model the closer the data points will fall to the fitted linear trend line.

From the sensitivity analysis, it was concluded that the coarse grid is unable to reproduce the hotspots modelled. As

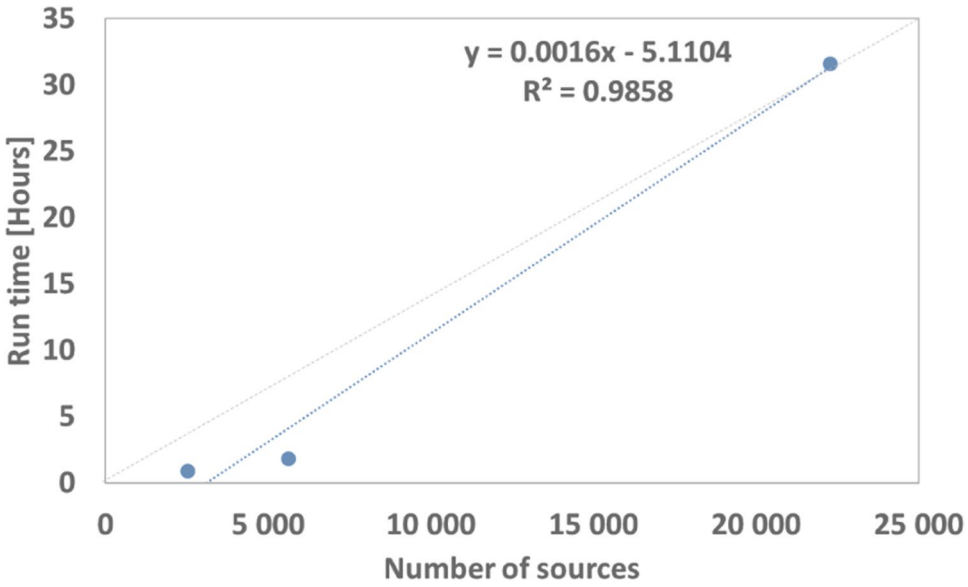

Fig. 8 Comparison between of computational time required and number of sources considered in URBAIR simulations for different mesh resolutions, for a daily simulation (24 h)

result of the small differences in the air pollutant concentrations between the medium and the fine mesh, both in terms of the magnitude of values and spatial pattern, and the time gained, it was argued that the medium grid is suitable to be used in the current study.

These results have a valuable role for future policy applications and long-term studies. The policy applications, for example, to study the impact of different mitigation measures or planning alternatives, usually have three main features: (i) a set of simulations are needed, since different scenarios are required to select the best solution/option to the problem under analysis; (ii) long-term analysis are required (1-year in an hourly basis) to cover a set of meteorological conditions; and (iii) larger areas are needed to take into account not only the city area but also its surroundings. All of these factors—several scenarios, long-term analysis and large areas—impact the computational power and time requirements. In other words, as higher the number of simulations, the time period and the number of cells, higher will be the computational power needed and the required computational time. To overcome these issues and give a timely response to decision-makers, a medium grid is recommended. Additionally, to explore, for example, the impact of climate change on air quality, which will imply that simulation of long series of meteorological data, the medium grid is also recommended. The finest grid should be used for short-term applications, for example, to simulate weather events and air quality episodes, or to model an area of interest (around 10 km × 10 km).

Model performance

As previously mentioned, the URBAIR model has been evaluated through time, showing good agreement between measurement and modelled data (Valente et al. 2014; Borrego et al. 2015, 2016; Dias et al. 2018). Despite of that, additional evaluation of the URBAIR model was carried out in this work.

The model accuracy was assessed by comparison of the modelled results (for a mesh resolution of 0.2×0.2 km^2) with the measurement data recorded at the automatic monitoring station located in the study area (see Fig. 2b), classified as background influence and as suburban environment, using as validation metrics the normalized parameters proposed by Chang and Hanna (2004). Table 3 points out the calculated statistic metrics for NO_2 and PM10 air pollutants, on an annual and seasonal basis. This evaluation was conducted in a daily average basis for PM10 and in an hourly basis for NO_2, accordingly the basis of the legislated limit values defined by Directive 2008/50/EC on ambient air quality and cleaner air for Europe. The air quality monitoring stations have a data collection efficiency of 98% and 92% during the simulation period, for PM10 and NO_2 respectively (around 2% of the daily PM10 measured data and 8% of the hourly NO_2 measured data were missing).

The correlation factor for the annual basis varies between 0.39 for NO_2 and 0.60 for PM10, denoting a good agreement between the measured and the modelled data, slightly better in the case of PM10, which one of the reasons that explain such results being the averaging times (daily average) of the PM10 statistics. This good agreement is so clear when the index of agreement is analysed; 0.63 and 0.72 were obtained for NO_2 and PM10, respectively. The index of agreement is sensitive to extreme values due to the squared differences, which can justify the good agreement. The NMSE values of 0.66 and 0.33 were obtained for NO_2 and PM10, respectively; this means that the NMSE acceptance criteria (ranges from 0 to 1.5) were fulfilled in the air quality station for NO_2

Table 3 Annual and seasonal statistical parameters for the assessment of modelling performance relative to the measurements. The evaluation was conducted in a daily average basis for PM10 and in an hourly basis for NO_2, accordingly the basis of the legislated limit values. Note: The statistical parameters definitions can be found in section 'Model evaluation'

		NMSE (−)	FAC2 (−)	*d* (−)	*r* (−)	RMSE (μg m^{-3})	MBE (μg m^{-3})
NO_2	Annual	0.66	0.63	0.63	0.39	9.78	+1.04
	Spring	1.30	0.45	0.41	0.06	11.78	−0.99
	Summer	0.69	0.70	0.51	0.31	8.45	+2.77
	Autumn	0.41	0.71	0.70	0.52	9.11	+1.11
	Winter	0.45	0.66	0.74	0.56	9.31	+1.35
PM10	Annual	0.33	0.77	0.72	0.60	15.54	+7.81
	Spring	0.36	0.73	0.54	0.43	13.34	+8.55
	Summer	0.72	0.69	0.35	0.14	18.97	+11.3
	Autumn	0.27	0.77	0.76	0.60	15.05	+5.01
	Winter	0.16	0.90	0.84	0.75	13.95	+6.25

and PM10. Regarding the MBE, which shows the tendency of the model to overestimate or underestimate a parameter, the model shows a clear tendency to overestimate both NO_2 and PM10 concentrations. An MBE of 1.04 μg m^{-3} was obtained for NO_2; for PM10, an MBE of 7.81 μg m^{-3} was obtained. The FAC2 results, which reflects the percentage of modelled results lying within a factor of two of the reference values (modelled results of the fine grid), showed that the acceptance criteria ($0.5 <= FAC2 <= 2.0$) suggested by Chang and Hanna (2004) are fulfilled for both PM10 (0.77) and NO_2 (0.63).

When the model performance is analysed seasonally (see Table 3), for both pollutants, a better performance is obtained for autumn and winter, i.e. the colder months, with a correlation factor varying between 0.52 and 0.56 for NO_2 and between 0.6 and 0.75 for PM10. Despite the overall overestimation of PM10 and NO_2 concentrations throughout the year, high values of MBE were obtained during spring and summer for both pollutants. These results highlight the role of meteorology and the uncertainties of emissions estimation in the model performance.

During the warmer season, i.e. summer, as the weather heats up, ground-level ozone is formed by the photochemical reaction of sunlight and NO_2. However, as URBAIR is a linear non-reactive model, this photochemical reaction is compromised, with NO_2 not being consumed, which leads to the highest overestimation of this pollutant. The overestimation of PM10 and NO_2 concentrations in the summer can also be explained by the prevailing wind direction and wind speed. During summer, wind roses show prevailing winds from NW, transporting pollutants directly from the main industrial areas to the location of the air quality monitoring station revealing an emission overestimation of this activity (SNAP 3/4). An underestimation of NO_2 concentration was obtained in spring (−0.99 μg m^{-3}). This result can be explained by the underestimation of the industrial (represents, in this season, on average 69% of the total emissions) and road transport emissions (represents, in this season, on average 22% of the total emissions) caused by the application of unsuitable European monthly profiles in the study region. In addition, since in the colder months the wind speed is higher than in the warmer months, higher dispersion of PM10 and NO_2 is promoted in winter and autumn, which can mask an emission overestimation. Nevertheless, the existence of only one air quality monitoring station can lead to a misinterpretation of the model's results.

Aiming to further investigate the model performance, measured *versus* modelled daily and hourly profiles were calculated. Figure 9 shows the hourly and daily profiles for NO_2 and PM10 concentrations, respectively.

The results show that the URBAIR model is able to reproduce the daily PM10 concentrations and the hourly NO_2 concentrations during the entire simulation period, with the model being able to catch trends of the pollutants simulated. However, the time series highlights the tendency to model overestimation, for both PM10 and NO_2 air pollutants, as concluded with the statistical analysis. For PM10, this overestimation has an impact on the exceedances' assessment. According to the URBAIR results, the PM10 daily limit value (50 μg m^{-3}) were exceeded in 41 days, while the air quality station registered 22 days where the daily limit was exceeded. This implies a difference between modelled and measured results of approximately 50%, which can be mainly justified, as previously mentioned, by an emission overestimation, particularly in the industrial sector. For NO_2, no exceedances to the hourly limit value (200 μg m^{-3}) were found for both data sources (modelled and measured). Based on the model performance results, it can be concluded that, as URBAIR is a linear non-reactive model, it is more suitable for PM, while there is some uncertainty in its results for other pollutants like NO_2 (Thunis et al. 2019), making URBAIR more appropriate to support air quality planning when the relation between emission and concentration changes remains linear.

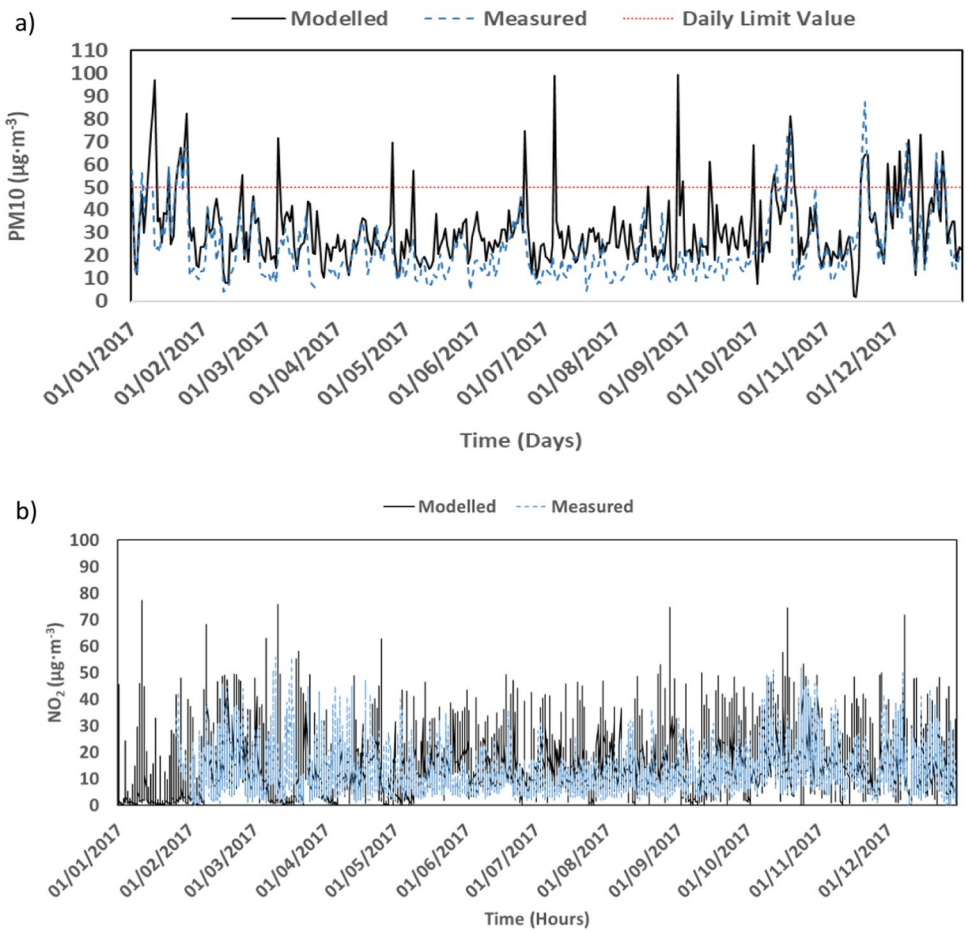

Fig. 9 Concentration profiles of measured and modelled values at 2017. **a** PM10 daily profile and **b** NO_2 hourly profile

Air quality assessment

The air quality characterization under the Estarreja area was conducted through two approaches: (i) maps with spatial distribution of the average concentrations for each season—spring (March–May), summer (June–August), autumn (September–November) and winter (December–February)—to determine the regions where pollution limits are exceeded; and (ii) source apportionment analysis, to identify the emission sources that are mainly responsible for the air pollution using as reference the location of the air quality station. Figures 10 and 11 show the spatial distribution of PM10 and NO_2 concentrations, respectively, by season. This analysis was made for a mesh resolution of 0.2 km (5330 receptor points), following the conclusions of the sensitivity analysis. Each analysis provides key factors for the formulation of regulatory actions and emissions reduction strategy.

The results show different spatial patterns according to the season and to the air pollutant analysed. The NO_2 concentrations show a strong correlation with the geographical locations of the main industrial areas and roads at all study periods. Other studies conducted in urban areas only relate the traffic emissions to high NO_2 concentration values (Vicente et al. 2018; Coelho et al. 2014). The local heating sources as well as the distributed industrial sources were the main contributors to the PM10 concentrations. Maximum PM10 and NO_2 concentrations were obtained in the summer period, with values of 70.6 µg m^{-3} and 63.2 µg m^{-3}, respectively; at the winter period, maximum values of 52.3 µg m^{-3} [NO_2] and 52.7 µg m^{-3} [PM10] were obtained. The maximum NO_2 concentrations were obtained across the main street roads and industrial areas, following the emissions spatial distribution and highlighting the contribution of the road traffic activity sector to the total NOx emissions (16.3% on average). The highest PM10 levels were obtained in the surroundings (in a 200-m radius) of the industrial sources with an annual emission less than 100 ton. Since the magnitude of emissions is very similar through the year, the differences obtained in terms of air pollutant concentrations are related with the meteorological conditions (wind speed and wind direction). During the summer, with the predominant wind direction coming from NW, the dispersion of pollutants follows the SE direction. However, as the intensity of the wind is predominantly weak to moderate, pollutant dispersion is low and the highest concentrations are obtained near the emission sources. In turn, in the winter,

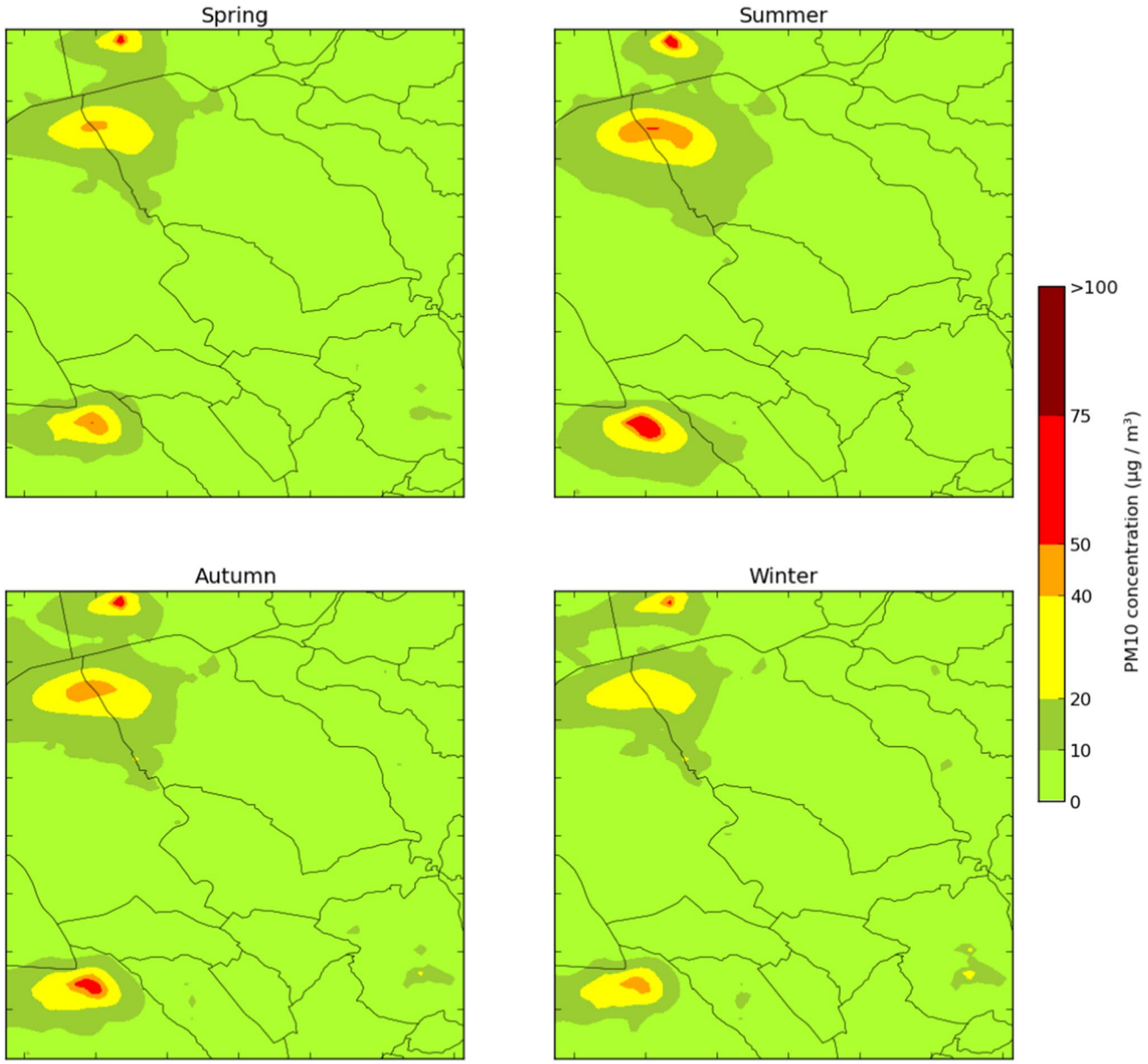

Fig. 10 Spatial distribution of PM10 average concentrations for each season: spring (March–May), summer (June–August), autumn (September–November) and winter (December–February)

as the wind intensity is higher (up to 18 m s^{-1}), there is a greater dispersion of pollutants, leading to lower concentration values. However, as there is no predominant wind direction, pollutants are almost equally dispersed in all directions. Values above the NO_2 annual limit value (40 µg m^{-3}) were obtained in 0.2% of the domain in the summer period (0.1% in winter); 1.2% of the domain registered values above the PM10 annual limit value (40 µg m^{-3}) in summer (0.2% in winter). Considering model results over the whole study domain in 2017, the spatial average concentrations of NO_2 ranges between 4.5 and 3.6 µg m^{-3}, for the summer and winter periods (the magnitude of NO_2 concentrations varies 0.2% between periods), respectively; the PM10 concentrations varies from 7.7 µg m^{-3} (summer) to 6.4 µg m^{-3} (winter). From the same results, the PM10 daily limit value (50 µg m^{-3}) was exceeded 45% of the days. In the case of NO_2 concentrations, values above the hourly limit value (200 µg m^{-3}) were not obtained.

Due to the linear approach of the URBAIR Gaussian model (where pollutant concentration is a summation of each source Gaussian contribution at a given location), it was possible to individually assess the contribution of each source to the overall concentration at any receptor point. This approach has been applied to assess the source

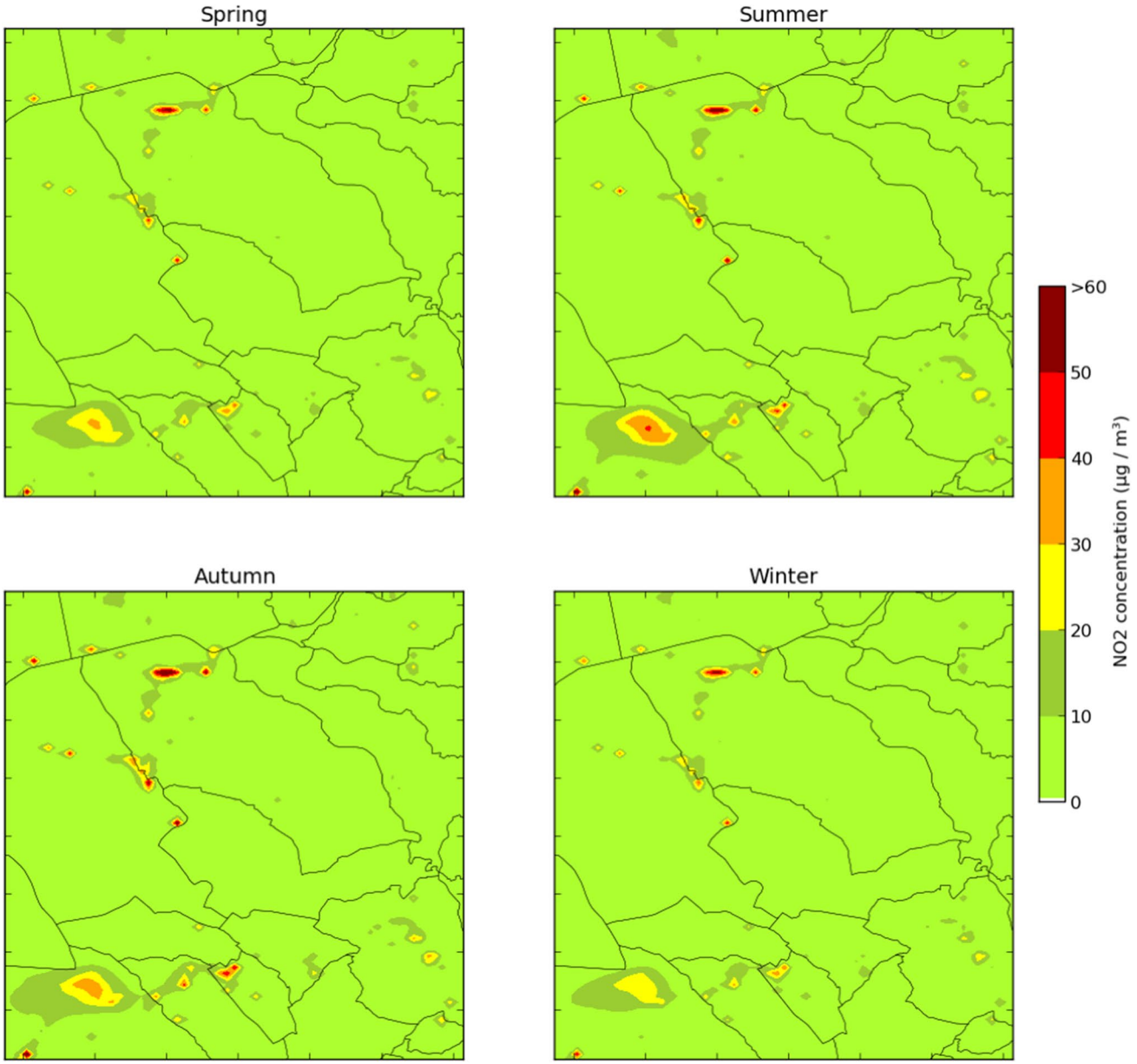

Fig. 11 Spatial distribution of NO_2 average concentrations for each season: spring (March–May), summer (June–August), autumn (September–November) and winter (December–February)

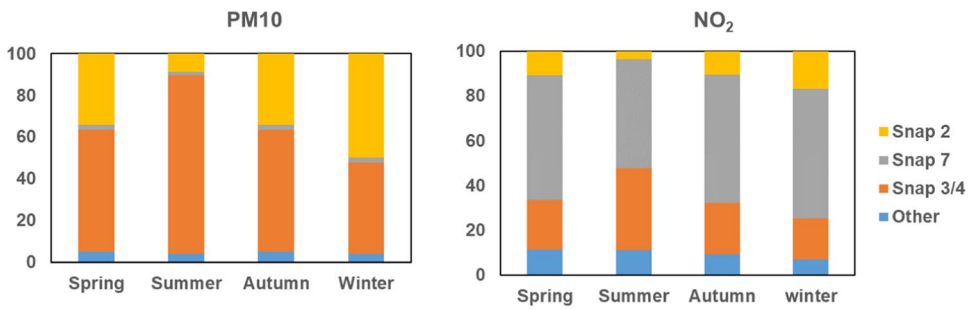

Fig. 12 Source apportionment assessment based on a season average concentration at air quality monitoring station location

apportionment at the selected receptor (location of the air quality station (see Fig. 2)). Figure 12 shows the source apportionment results for PM10 and NO_2 pollutants for each season.

To assess the importance of each sector in the source apportionment analysis, the average of the relative contributions of each pollutant was considered. Thus, for the average of the two pollutants, on an annual basis, industrial combustion and processes (SNAP 3/4) present the most important activity, with an average contribution of 44%, followed by road transport (SNAP 7) with 28%, residential and commercial combustion (SNAP 2) with 21%, and the Others with only 7%. According to Fig. 12, for both PM10 and NO_2, SNAP 3/4 highest contributions are recorded in summer, with a maximum of 86% for PM10 and 37% for NO_2, and the lowest in winter (44% for PM10 and 18% for NO_2). These results are related to the location of the air quality monitoring station, at the SE of the industrial areas of Estarreja and Avanca, and with prevailing winds from NW, especially during the summer (Figs. 3 and 4). Another activity with a relevant contribution is road transport (SNAP 7), being the activity that represents the highest contributions for NO_2, with values varying between 49% (summer) and 58% (winter). In turn, for PM10, SNAP 7 represents a contribution of only 2%, throughout the year. These results show the relation between road traffic and NO_2 concentrations, further evidenced by the proximity between the air quality monitoring station and some of the busiest roads in the region, which are in accordance with the conclusions of previous studies (Vicente et al. 2018; Coelho et al. 2014). Residential and commercial combustion (SNAP 2) is the third most important activity, mainly influencing PM10 concentrations, especially during winter, when it reaches to values of 50%, suggesting a greater use of residential wood combustion during cold months (Gama et al. 2018). For NO_2, SNAP 2 only represents 4% in summer and 17% in winter. Finally, the remaining activities (Other) do not exceed 11% (5%) contribution to the NO_2 (PM10) seasonal average concentrations.

Although these results are an asset in identifying the main sources of atmospheric emissions, their use for air quality management purposes should be done with caution. As stated by Thunis et al. (2019), source apportionment analysis using a linear non-reactive model, as URBAIR, is appropriate to estimate sectoral contributions to support air quality management only when emission-concentration relation remains linear. In case of non-linear processes, like chemical transformations and non-linear interactions between the sources, effective air quality management policies are not necessarily the ones tackling the most dominant emission source but those tackling the substance that is most scarce or binding in the pollution formation. In these cases, emission reduction scenarios, for the identified activity sectors, must also be tested. Despite of that, this kind of analysis provides a diagnosis of air quality issues, which provides useful information on the contribution of sources that can be controlled (anthropogenic sources) versus uncontrollable sources, such as boundary conditions and biogenic emissions. This information can be used as part of the decision-making process (along with economic, political and societal considerations) by policy makers in efforts to identify effective mitigation measures to improve air quality.

Conclusions

Gaussian approaches have been used on atmospheric dispersion modelling to assess the air pollution levels and provide technical/scientific support to the decision-makers. In this sense, the main goal of this work was to perform a sensitivity analysis of URBAIR, a second-generation Gaussian model, focused on impact of different spatial resolutions on output results and evaluate its accuracy to simulate air pollution patterns in urban areas. The Estarreja area, a city located near four industrials facilities, was used as case study.

To accomplish the proposed goal, three different grid resolutions were investigated: 0.1 km (fine grid), 0.2 km (medium grid) and 0.3 km (coarse grid). Please note that the type of approach, level of complexity and purposes of a sensitivity analysis vary significantly depending on the modelling domain and the specific application aims. The comparative analysis allowed to conclude that small differences were obtained between the three grids, regarding the spatial distribution of PM10 and NO_2 concentrations across the study area, as well as in terms of the concentration magnitude. These results are explained by the non-chemistry reactive approach of the URBAIR Gaussian approach, which implies that only the emissions spatial resolution contributes to the discrepancies of the model outputs. However, an increase of the computational time by approximately 1.5 times for the medium grid (0.2 km) and 13 times more for the fine grid (0.1 km) was found when compared with the coarse grid (0.3 km). For a compromise between accurate results and computational time demand, the URBAIR model was applied for the 2017 year with a mesh resolution of resolution 0.2×0.2 km^2 and an hourly run time step, to explore the ability of URBAIR model to be a tool that supports decision-makers in urban air quality management.

First, the performance of URBAIR model was assessed. Overall, the URBAIR model is able to reproduce the PM10 and NO_2 concentrations, which is in accordance with previous works. However, the time series highlights the trend to model overestimation, for both PM10 and NO_2 air pollutants. Second, an air quality characterization of the study area was conducted. The analysis of the spatial patterns revealed that the maximum NO_2 concentrations were obtained near the main roads and industrial areas, following the spatial

emission distribution patterns and the contribution of the surrounding activities to the total emissions. Particularly, the highest PM10 levels were obtained in the surroundings of the industrial sources. This analysis was complemented with a source apportionment assessment at the location of the available air quality monitoring station. The results showed that the road transport sector (SNAP 7) is the activity that contributes the most to NO_2 concentrations, with values varying between 49% (summer) and 58% (winter). For PM10, the most important sector is the industrial combustion and processes (SNAP 3/4), for all seasons, with contributions ranging from 44% during winter to 86% in summer.

The URBAIR performance assessment shows that the air quality model provides reliable numerical simulations for particles and gaseous atmospheric pollutants at the city level with high spatial and temporal resolutions as well as small computational and time requirements. These results demonstrate the utility of this numerical tool to help and provide technical/scientific support to the policy makers on identification of the responsibility of atmospheric emission sources in high air pollution levels in urban areas and therefore on definition of efficient urban planning alternatives, through source apportionment, to reduce the human exposure to air pollution and its health effects.

Funding The authors acknowledge the financial support of FEDER through the COMPETE Programme and the national funds from FCT – Science and Technology Portuguese Foundation within the project InFLOWence (POCI-01–0145-FEDER-029679) and the Ph.D grants of S. Coelho (SFRH/BD/137999/2018). Thanks are due for the financial support to CESAM (UIDB/50017/2020 + UIDP/50017/2020), to FCT/MCTES through national funds, and the co-funding by the FEDER, within the PT2020 Partnership Agreement and Compete 2020. Thanks are also due to FCT/MCTES for the contract granted to Sandra Rafael (2020.02543.CEECIND).

Data availability The data that support the findings of this study are available from the corresponding author upon reasonable request.

References

Benson PE (1989) CALINE 4: a dispersion model for predicting air pollutant concentrations near roadways, FHWA-CA-TL-84–15. California Department of Transportation, Sacramento, CA, USA

Borrego C, Martins JM, Lemos S, Guerreiro C (1997) A second generation Gaussian dispersion model: the POLARIS model. Int J Environ Pollut 8:789–795. https://doi.org/10.1504/IJEP.1997.028232

Borrego C, Lopes M, Cascão P, Amorim JH, Martins H, Tavares R, Miranda AI, Tallis MJ, Freer-Smith PH (2015) Chapter 8: urban air quality models. In: Chrysoulakis N, Castro EA, Moors EJ (eds) Understanding urban metabolism: a tool for urban planning, 1st edn. Taylor & Francis, London, pp 256

Borrego C, Amorim JH, Tchepel O, Dias D, Rafael S, Sa E, Pimentel C, Fontes T, Fernandes P, Pereira SR, Bandeira JM, Coelho MC (2016) Urban scale air quality modelling using detailed traffic emissions estimates. Atmos Environ 131:341–351. https://doi.org/10.1016/j.atmosenv.2016.02.017

Carruthers DJ, Holroyd RJ, Hunt JCR, Weng WS, Robins AG, Apsley DD, Thompson DJ, Smith FB (1994) UK-ADMS: a new approach to modelling dispersion in the earth's atmospheric boundary layer, Journal of Wind Engineering and Industrial Aerodynamics, 52. ISSN 139–153:0167–6105. https://doi.org/10.1016/0167-6105(94)90044-2

Chang J, Hanna S (2004) Air quality model performance evaluation. Meteorol Atmos Phys 87:167–196. https://doi.org/10.1007/s00703-003-0070-7

Chrysoulakis N, Lopes M, San JR, Grimmong CSB, Jones MB, Magliulo V, Klostermann JE, Mitraka Z, Castro EA, González A, Vogt R, Vesala T, Spano D, Pigeon G, Freer-Smith P, Staszewski T, Hodges N, Mills G, Cartalis C (2013) Sustainable urban metabolism as a link between bio-physical sciences and urban planning: the BRIDGE project. Landsc Urban Plan 112:100–117. https://doi.org/10.1016/j.landurbplan.2012.12.005

Cimorelli AJ, Perry SG, Venkatram A, Weil JC, Paine RJ, Wilson RB, Lee RF, Peters WD, Brode RW (2005) AERMOD: a dispersion model for industrial source applications. Part I: General model formulation and boundary layer characterization. J Appl Meteor 44:682–693. https://doi.org/10.1175/JAM2227.1

Coelho MC, Fontes T, Bandeira J, Pereira S, Tchepel O, Sá E, Amorim JH, Borrego C (2014) Assessment of potential improvements on regional air quality modelling related with implementation of a detailed methodology for traffic emissions estimation. Sci Total Environ 470:127–137. https://doi.org/10.1016/j.scitotenv.2013.09.042

DGT (Direção Geral do Território) (2018) Cartografia de Uso e Ocupação do Solo (COS, CLC e Copernicus) [WWW Document]. http://www.dgterritorio.pt. Accessed 10 Oct 2020

Dias D, Amorim JH, Sa E, Borrego C, Fontes T, Fernandes P, Pereira SR, Bandeira J, Coelho MC, Tchepel O (2018) Assessing the importance of transportation activity data for urban emission inventories. Transp Res D Trans Environ 62:27–35. https://doi.org/10.1016/j.trd.2018.01.027

Dudhia J (1989) Numerical study of convection observed during the winter monsoon experiment using a mesoscale two-dimensional model. J Atmos Sci 46(20):3077–3107. https://doi.org/10.1175/1520-0469(1989)046%3c3077:NSOCOD%3e2.0.CO;2

EEA (2019) Air quality in Europe—2019 report. European Environment Agency, Copenhagen. No 10/2019. https://doi.org/10.2800/822355. https://www.eea.europa.eu/publications/air-quality-in-europe-2019. Accessed 19 Dec 2020

EMEP (European Monitoring and Evaluation Programme) (2017) European monitoring and evaluation programme [WWW Document]. http://www.emep.int/. Accessed 12 Sept 2020

Fernandes P, Vilaca M, Macedo E, Sampaio C, Bahmankhah B, Bandeira JM, Guarnaccia C, Rafael S, Fernandes AP, Relvas H, Borrego C, Coelho MC (2019) Integrating road traffic externalities through a sustainability indicator. Sci Total Environ 691:483–498. https://doi.org/10.1016/j.scitotenv.2019.07.124

Fernández J, Montávez J, Sáenz J, González-Rouco J, Zorita E (2007) Sensitivity of the MM5 mesoscale model to physical parameterizations for regional climate studies: annual cycle. J Geophys Res 112D4 D04101, https://doi.org/10.1029/2005JD006649

Fountoukis C, Koraj D, Denier van der Gon HAC, Charalampidis PE, Pilinis C, Pandis SN (2013) Impact of grid resolution on the predicted fine PM by a regional 3-D chemical transport model. Atmos Environ 68:24–32. https://doi.org/10.1016/j.atmosenv.2012.11.008

Gama C, Monteiro A, Pio C, Miranda AI, Baldasano JM, Tchepel O (2018) Temporal patterns and trends of particulate matter over Portugal: a long-term analysis of background concentrations.

Air Qual Atmos Health 11:397–407. https://doi.org/10.1007/s11869-018-0546-8

Garcia-Menendez F, Odman MT (2011) Adaptive grid use in air quality modeling. Atmosphere 2(484–509):10. https://doi.org/10.3390/atmos2030484

Gon HD, van der Hendriks C, Kuenen J, Segers A, Visschedijk A (2011) TNO report description of current temporal emission patterns and sensitivity of predicted AQ for temporal emission patterns. EU FP7 MACC deliverable report D_D-EMIS_1.3. https://atmosphere.copernicus.eu/sites/default/files/2019-07/MACC_TNO_del_1_3_v2.pdf. Accessed 12 Sept 2020

Grell GA, Dévényi D (2002) A generalized approach to parameterizing convection combining ensemble and data assimilation techniques. Geophys Res Lett 29(14):1693. https://doi.org/10.1029/2002GL015311

Gulia S, Kumar A, Khare M (2015) Performance evaluation of CALPUFF and AERMOD dispersion models for air quality assessment of an industrial complex. J Sci Ind Res 74: 302–307. Link: http://nopr.niscair.res.in/bitstream/123456789/31451/1/JSIR%2074%285%29%20302-307.pdf

Hong SY, Dudhia J, Chen SH (2004) A revised approach to ice microphysical processes for the bulk parameterization of clouds and precipitation. Mon Wea Rev 132(1):103–120. Link: https://pdfs.semanticscholar.org/87f9/038cd23d30dbb19541c1c6bcec83f4987d6d.pdf

Hong SY, Noh Y, Dudhia J (2006) A new vertical diffusion package with an explicit treatment of entrainment processes. Mon Wea Rev 134:2318–2341. https://doi.org/10.1175/MWR3199.1

INE (Instituto Nacional de Estatística) (2011) Statistics Portugal, 2011. CENSUS, 2011- statistical data for Portugal [WWW Document]. http://censos.ine.pt. Accessed 11 April 2020

Kewo A, Manembu P, Nielsen P (2020) Synthesising residential electricity load profiles at the city level using a weighted proportion (Wepro) model. Energies 13:3543. https://doi.org/10.3390/en13143543

Li X, Lopes D, Mok KM, Miranda AI Yuen KV (2019) Development of a road traffic emission inventory with high spatial – temporal resolution in the world' s most densely populated region — Macau Environ Monit Assess 191–239. https://doi.org/10.1007/s10661-019-7364-9

Lopes D, Ferreira J, Hoi KI, Miranda AI, Yuen KV, Mok KM (2019) Weather research and forecasting model simulations over the Pearl River Delta Region. Air Qual Atmos Health 12(1):115–125. https://doi.org/10.1007/s11869-018-0636-7

Ma J, Yi H, Tang X, Zhang Y, Xiang Y, Pu L (2013) Application of AERMOD on near future air quality simulation under the latest national emission control policy of China: a case study on an industrial city. J Environ Sci 25:1608–1617. https://doi.org/10.1016/S1001-0742(12)60245-9

Mlawer EJ, Taubman SJ, Brown PD, Iacono MJ, Clough SA (1997) Radiative transfer for inhomogeneous atmospheres: RRTM, a validated correlated-k model for the longwave. J Geophys Res Atmos 102(D14):16663–16682. https://doi.org/10.1029/97JD00237

Mocerino L, Murena F, Quranta F, Toscano D (2020) A methodology for the design of an effective air quality monitoring network in port areas. Sci Rep 10:300. https://doi.org/10.1038/s41598-019-57244-7

Oleniacz R, Rzeszutek M (2018) Intercomparison of the CALMET/CALPUFF modeling system for selected horizontal grid resolutions at a local scale: a case study of the MSWI plant in Krakow. Poland Appl Sci 8:1–19. https://doi.org/10.3390/app8112301

OpenStreetMap contributors (2017) Planet dump [Data file from $date of database dump$]. Retrieved from https://www.planet.openstreetmap.org [WWW Document]. Accessed 02 Oct 2020

Pianosi F, Beven K, Freer J, Hall J, Rougier J, Stephenson D, Wagener T (2016) Sensitivity analysis of environmental models: a systematic review with practical workflow. Environ Model Softw 79:214–232. https://doi.org/10.1016/j.envsoft.2016.02.008

Rafael S, Martins H, Sa E, Carvalho D, Borrego C, Lopes M (2016) Influence of urban resilience measures in the magnitude and behaviour of energy fluxes in the city of Porto (Portugal) under a climate change scenario. Sci Total Environ 566:1500–1510. https://doi.org/10.1016/j.scitotenv.2016.06.037

Rafael S, Martins H, Marta-Almeida M, Sa E, Coelho S, Rocha A, Borrego C, Lopes M (2017) Quantification and mapping of urban fluxes under climate change: application of WRF-SUEWS model to Greater Porto area (Portugal). Environ Res 155:321–334. https://doi.org/10.1016/j.envres.2017.02.033

Rafael S, Vicente B, Rodrigues V, Miranda AI, Borrego C, Lopes M (2018) Impacts of green infrastructures on aerodynamic flow and air quality in Porto's urban area. Atmos Environ 190:317–330. https://doi.org/10.1016/j.atmosenv.2018.07.044

Rafael S, Rodrigues V, Fernandes AP, Augusto B, Borrego C, Lopes M (2019) Evaluation of urban surface parameterizations in WRF model using energy fluxes measurements in Portugal. Urban Clim 28, https://doi.org/10.1016/j.uclim.2019.100465

Rafael S, Martins H, Matos MJ, Cerqueira M, Pio C, Lopes M, Borrego C (2020) Application of SUEWS model forced with WRF: energy fluxes validation in urban and suburban Portuguese area. Urban Clim 33, https://doi.org/10.1016/j.uclim.2020.100662

Rafael S, Rodrigues V, Oliveira K, Coelho S, Lopes M (2021) How to compute long-term averages for air quality assessment at urban areas? Sci. Total Environ. (2021), Article number 148603. https://doi.org/10.1016/j.scitotenv.2021.148603

Schulman LL, Strimaitis DG, Scire JS (2000) Development and evaluation of the PRIME plume rise and building downwash model. J Air Waste Manag Assoc 50:378–390. https://doi.org/10.1080/10473289.2000.10464017

Scire JS, Strimaitis DG, Yamartino RJ (1990a) Model formulation and user's guide for the CALPUFF dispersion model. Sigma Research Corporation, Concord, MA. Available from http://www.src.com/CALPUFF/download/CALPUFF_UsersGuide.pdf

Scire JS, Insley EM, Yamartino RJ (1990b) Model formulation and user's guide for the CALMET meteorological model. Sigma Research Corporation, Concord, MA. Available from https://www.arpae.it/cms3/documenti/_cerca_doc/meteo/ambiente/manuale_calmet.pdf

Silveira C, Ferreira J, Monteiro A, Miranda AI, Borrego C (2017) Emissions from residential combustion sector: how to build a high spatially resolved inventory. Air Qual. Atmos. Health., 1–12. https://doi.org/10.1007/s11869-017-0526-4

Skamarock WC, Klemp JB, Dudhia J, Gill DO, Barker DM, Duda MG, Huang XY, Wang W, Powers JG (2008) A description of the advanced research WRF version 3 NCAR/TN-475+STR. Boulder, Colorado, USA. https://doi.org/10.5065/D68S4MVH

Taghavi M, Cautenet S, Arteta J (2005) Impact of a highly detailed emission inventory on modeling accuracy. Atmos Res 74:65–88. https://doi.org/10.1016/j.atmosres.2004.06.007

Tavares R, Miranda AI, Borrego C (2011) Modelling and assessing risks from accidental release of hazardous gases. Second international Conference on Air Pollution and Control, 19 - 23 September, Antalya, Turquia.

Tchepel O, Dias D, Ferreira J, Tavares R, Miranda AI, Borrego C (2012) Emission modelling of hazardous air pollutants from road transport at urban scale. Transport 27(3):299–306. https://doi.org/10.3846/16484142.2012.720277

Tewari M, Chen F, Wang W, Dudhia J, LeMone MA, Mitchell K, Ek M, Gayno G, Wegiel J, Cuenca RH (2004) Implementation and verification of the unified NOAH land surface model in the WRF model. In 20th Conference on Weather Analysis and Forecasting/16th Conference on Numerical Weather Prediction. pp. 11–15

Thunis P, Clappier A, Tarrason L, Cuvelier C, Monteiro A, Pisoni E, Wesseling J, Belis CA, Pirovano G, Janssen S, Guerreiro C, Peduzzi E (2019) Source apportionment to support air quality planning: strengths and weaknesses of existing approaches. Environ Int 130:104825. https://doi.org/10.1016/j.envint.2019.05.019

Truong S, Lee MI, Kim G, Kim D, Park JH, Choi SD, Cho GH (2016) Accidental benzene release risk assessment in an urban area using an atmospheric dispersion model. Atmos Environ 144:146–159. https://doi.org/10.1016/j.atmosenv.2016.08.075

United Nations (2015) Sustainable development goals: 17 goals to transform our world. Available from https://www.un.org/sustainabledevelopment/sustainable-development-goals/

Valente J, Pimentel C, Tavares R, Ferreira J, Borrego C, Carreiro-Martins P, Caires I, Neuparth N, Lopes M (2014) Individual exposure to air pollutants in a Portuguese urban industrialized area. J Toxicol Environ Heal Part A 77:888–899. https://doi.org/10.1080/15287394.2014.910159

Vicente B, Rafael S, Rodrigues V, Relvas H, Vilaça M, Teixeira J, Bandeira J, Coelho M, Borrego C (2018) Influence of different complexity levels of road traffic models on air quality modelling at street scale. Air Qual Atmos Health 11:1217–1232. https://doi.org/10.1007/s11869-018-0621-1

Wang X, Zhang L, Moran MD (2014) Development of a new semi-empirical parameterization for below-cloud scavenging of size-resolved aerosol particles by both rain and snow. Geosci Model Dev 7:799–819. https://doi.org/10.5194/gmd-7-799-2014

Weil JC, Corio LA, Brower RP (1997) A PDF dispersion model for buoyant plumes in the convective boundary layer. J Appl Meteor 36:982–1003. https://doi.org/10.1175/1520-0450(1997)036%3c0982:APDMFB%3e2.0.CO;2

Willmott CJ (1981) On the validation of models. Phys Geogr 2:184–194. https://doi.org/10.1080/02723646.1981.10642213

Wu H, Zhang Y, Yu Q, Ma W (2018) Application of an integrated Weather Research and Forecasting (WRF)/CALPUFF modeling tool for source apportionment of atmospheric pollutants for air quality management: a case study in the urban area of Benxi, China. J Air Waste Manag Assoc 68(4):347–368. https://doi.org/10.1080/10962247.2017.1391009

Zhang D, Anthes RA (1982) A high-resolution model of the planetary boundary layer—sensitivity tests and comparisons with SESAME-79 data. J Appl Meteor 21:1594–1609. https://doi.org/10.1175/1520-0450(1982)021%3c1594:AHRMOT%3e2.0.CO;2